The hydrodynamic limit for dense nitrogen and argon gases

1992 J. Phys.: Condens. Matter 4 8945

(http://iopscience.iop.org/0953-8984/4/46/002)

J. Phys.: Condens. Matter 4 (1992) 8945–8960. Printed in the UK

The hydrodynamic limit for dense nitrogen and argon gases

J Youden†, P A Egelstaff†, J Mutka‡ and J-B Suck‡

† Guelph–Waterloo Program for Graduate Work in Physics, Guelph Campus, University of Guelph, Guelph, Ontario, Canada N1G 2W1

‡ Institut Laue–Langevin, Avenue des Martyrs, Grenoble 38042, France

Received 2 July 1992

Abstract. The behaviour of the coherent scattering function, $S(Q, \omega)$ (where $\hbar Q$ and $\hbar\omega$ are the momentum and energy transferred in radiation scattering experiments) in the limit of small Q approaching the hydrodynamic limit has been discussed in many theoretical papers. However, experimental results have mainly been confined to liquid metals and near-quantum fluids. With the new experimental arrangement described by Egelstaff and co-workers in 1989 such experiments have been extended to dense classical gases, and can complement light scattering experiments where this limit is reached in dilute gases. This paper describes the observed behaviour of $S(Q, \omega)$ as Q is increased away from the hydrodynamic region, for a dense gas sample at constant density. The data are compared to theoretical predictions, for which there are essentially no adjustable parameters, and the region where the theory is successful as well as the initial departures from it are identified.

1. Introduction

The density fluctuations in a fluid that occur on a macroscopic scale can be described by the equations of linearized hydrodynamics. Such fluctuations may be discussed conveniently through the van Hove space–time correlation function $G(r, t)$ (Boon and Yip 1980). This function may be studied through radiation scattering experiments, which yield the Fourier transform of $G(r, t)$, namely $S(Q, \omega)$ where Q and ω are the transform variables for r and t respectively and where $\hbar Q$ and $\hbar\omega$ are the momentum and energy transferred by the radiation to the fluid (van Hove 1954). In the case of inelastic light scattering experiments the scattered frequency spectrum for samples of a gas may be studied at relatively small values of Q, and over a wide range of densities. It is found that the classical theory of hydrodynamics can describe the data at high density and departures from it are observed at low density. In the case of neutron inelastic scattering a complementary and more basic experiment is possible, in which the scattering experiments are conducted at a single high density and departures from hydrodynamic theory are observed as Q is increased from the $Q \to 0$ limit to values comparable to $2\pi/Q \approx$ the intermolecular spacing at this density.

Specifically for hard-sphere fluids the hydrodynamic equations are valid in the region for which the wavelength and the time scale of the density fluctuations are much greater than, respectively, the mean free path (l), and the time between collisions (τ). In terms of the dimensionless length and frequency parameters y and x (Nelkin and Yip 1966), where $y = (\sqrt{2}Ql)^{-1}$, $x = \omega(\sqrt{2}Qv_0)^{-1}$, and

0953-8984/92/468945+16$07.50

$v_0 = (k_B T/M)^{1/2}$ is the thermal velocity, this limit is $\omega\tau \ll 1$ and $Ql \ll 1$ or $x \ll y$ and $y \gg 1$ respectively. For the transition region of $y \sim 1$ and $x/y \sim 1$ the hydrodynamic equations are no longer strictly valid due to the influence of the microscopic structure. The form of the hydrodynamic equations can, however, be extended over a larger Q region through the generalization of the thermodynamic and transport coefficients to functions of Q and/or ω (Mountain 1976). Models of this kind have been described for example by Chung and Yip (1969), Sears (1970), Ailawadi *et al* (1971), and Mountain (1976), with further discussions contained in Boon and Yip (1980). Thus as Q is increased from the $Q \to 0$ limit to the region where x/y and $y \sim 1$ it is of interest to observe how the hydrodynamic theory fails, and study the form of elementary excitations of high frequency (e.g. Zwanzig 1967). Our new experimental apparatus has been described in an initial publication (Egelstaff *et al* 1989), and here we describe both some experimental improvements and the analysis and interpretation of the new data.

Among the initial studies of the behaviour of noble gases in the transition regime were those of Clark (1975), who used inelastic light scattering measurements on dilute xenon gas. By varying the density of the sample, and hence its mean free path, it was possible to go from the hydrodynamic region of $y > 6$ to the kinetic region of $y < 1$. In the case of neutron inelastic scattering Bell *et al* (1973, 1975) obtained experimental data for the density fluctuations in neon in the regions $0.6 < Q < 1.4$ nm^{-1} and $2.7 < Q < 15.0$ nm^{-1}. In the lower Q-range the data were consistent with linearized hydrodynamics, whereas for higher Q generalizations of the macroscopic coefficients were required, mainly through a Q-dependence in the thermal diffusivity D_T, and a (Q, ω)-dependence in the longitudinal viscosity. In addition, the density fluctuations in dense argon in the region $1 < Q < 6$ nm^{-1} have been measured by Postol and Pelizzari (1978), with comparisons being made to the generalized Enskog kinetic theory. In many of these neutron measurements the quality of the data was limited by relatively low intensities and poor resolution relative to the width of the peaks, which meant that clearly defined lines were not seen in the raw data.

Propagating collective modes can be observed at significantly higher Q-values in some other fluids. The existence of such modes in liquid metals is quite well known, and in particular liquid rubidium (Copley and Rowe 1974a, b) and liquid lead (Söderström *et al* 1980) have been studied extensively. In rubidium for Q up to 12 nm^{-1}, distinct peaks have been observed both in the real fluid and in a simulation via molecular dynamics (Rahman 1974a, b). In normal liquid helium sound mode peaks at low Q have been measured by, for example, Dasannacharya *et al* (1976), and Woods *et al* (1978a, b). In addition, collective excitations in liquid parahydrogen have been observed by Carneiro *et al* (1973).

While the wavelength and time scales which are examined by molecular dynamics (MD) computer simulations are generally of the order of molecular length and time scales, studies of the collective effects in fluids at relatively long wavelengths have been made also. For example, the Lennard-Jones fluid has been studied by Levesque *et al* (1973), and hard-sphere fluids by Alley and Alder (1983) and Alley *et al* (1983). In both these fluids, the spectra could be described by generalized hydrodynamic models. In addition, the latter study delineates the regions where the hydrodynamic and generalized Enskog kinetic theories are valid for a hard-sphere fluid, as well as—in the regions where a generalization of hydrodynamics is required—specifying the necessary dependences of the generalized coefficients.

Recently, much work has been done on the extended hydrodynamic model (see,

for example, de Schepper and Cohen (1980), van Well and de Graaf (1985), and the references therein), in which $S(Q, \omega)$ is given by the first three terms of an infinite sum of Lorentzians which is the kinetic theory description $S(Q, \omega)$ for a system of hard spheres. Analyses with this theory have covered the intermediate Q-range of roughly 3 to 40 nm^{-1}, where experimental data on liquid argon (de Schepper *et al* 1983), and liquid and dense fluid neon (van Well and de Graff 1985), as well as MD simulations for a Lennard-Jones fluid (de Schepper *et al* 1984), can be fitted by the generalized three-Lorentzian form. Recent measurements on argon gas (Bafile *et al* 1990) using the technique described by Egelstaff *et al* (1989), at the low Q-values of 0.5 to 1.3 nm^{-1} have been interpreted in this way, and we shall discuss these data in section 5.

Recent modifications (see section 3) which we have made to the IN5 neutron spectrometer at the Institut Laue–Langevin have permitted low-Q inelastic scattering experiments to be performed readily, thereby enabling a systematic study of the collective fluctuations in dense fluids to be started. In the present initial phase, the dynamic structure factor $S(Q, \omega)$ for fluid nitrogen (at 1.3 and 0.9 of the critical density) was measured in the low Q-range—from the upper limit of hydrodynamics, to the largest Q-values available at this time. The experimental $S(Q, \omega)$ functions are interpreted within this framework of the generalized hydrodynamic models, in order to explore the first deviations from the macroscopic theory.

In addition we shall interpret some of the results obtained by Bafile *et al* (1990) in the same way. Thus these results fall in the region between the collective fluctuations on a macroscopic scale as measured through light scattering experiments, and the region of molecular behaviour that is accessible within the more conventional Q-range of neutron scattering and MD simulations.

2. Hydrodynamic theory and generalizations

The long-wavelength fluctuations in a fluid may be described through linearized hydrodynamics, which yields for the dynamic structure factor (Boon and Yip 1980)

$$\frac{S(Q, \omega)}{S(Q)} = \frac{1}{\pi} \operatorname{Re} \lim_{\epsilon \to 0} \frac{s^2 + s(\nu_l + \gamma\chi)Q^2 + \nu_l\gamma\chi Q^4 + (1 - \gamma^{-1})c^2Q^2}{s^3 + s^2(\nu_l + \gamma\chi)Q^2 + s(\nu_l\gamma\chi Q^4 + c^2Q^2) + \chi c^2Q^4} \tag{1}$$

where $s = \epsilon + i\omega$, ν_l is the longitudinal kinematic viscosity, χ is the thermal diffusivity or $\lambda/M_\rho C_p$ where λ is thermal conductivity, M is the particle mass, ρ is the number density, and C_p the specific heat at constant pressure, c is the velocity of sound and γ is the ratio of specific heats. In the low Q-range where the widths (i.e. damping processes) associated with the hydrodynamic modes are small compared to the shift $\omega = cQ$ of the propagating mode, one may approximate the roots of the denominator in the above equation by their lowest-order expressions. The resulting expression for $S(Q, \omega)$ thus consists of three Lorentzians—a central entropy fluctuation mode, and two propagating acoustic modes—as well as two S-shaped terms centred at $\omega = \pm cQ$. These latter two terms become negligible in the limit of Q tending to zero. However, at larger Q where the widths of the spectra are no longer small compared to the shifts, the higher-order terms become important, so the entire expression (1) must be used.

To study the deviations between the linearized hydrodynamics theory and the structure of a real fluid in the transition region of intermediate wavelengths and

frequencies, it is convenient to generalize the coefficients appearing in $S(Q, \omega)$—Kadanoff and Martin (1963), and Sears (1969, 1970). For convenience we use the expression for $S(Q, \omega)$ in terms of the memory function $M(Q, \omega)$ (Boon and Yip 1980)

$$\frac{S(Q, \omega)}{S(Q)} = \frac{1}{\pi} \frac{\omega_0^2 Q^2 M'}{[(\omega^2 - \omega_0^2 + \omega Q^2 M'')^2 + (\omega Q^2 M')]^2} \tag{2a}$$

with

$$\omega_0^2 = (k_B T / M S(Q)) Q^2 \to Q^2 / M \rho \chi_T = (c^2/\gamma) Q^2 \qquad \text{as } Q \to 0 \tag{2b}$$

where χ_T is the isothermal compressibility and $S(Q)$ is the static structure factor. In the low-Q limit $M(Q, \omega)$—from the solution of the linearized hydrodynamic equations—has the real and imaginary parts

$$M'(Q, \omega) = (1 - \gamma^{-1}) c^2 \gamma \chi Q^2 / [(\gamma \chi)^2 Q^4 + \omega^2] + \nu_1 \tag{3a}$$

$$M''(Q, \omega) = -\omega (1 - \gamma^{-1}) c^2 / [(\gamma \chi)^2 Q^4 + \omega^2]. \tag{3b}$$

While equation (2) is formally valid for all Q and ω, the choice (3a) and (3b) of the memory function restricts its applicability to the long-wavelength, low-frequency region characteristic of hydrodynamics. This case reduces to equation (1) if the $Q \to 0$ limit in (2b) is used. In the transition region of Q- and ω-space where the microscopic structure of the fluid influences the relaxation processes in a manner different from that given by the macroscopic limit of the thermodynamic and transport coefficients, generalizations of the hydrodynamic description consist of writing these coefficients as functions of Q and/or ω (see, for example, Mountain 1976). For example, the simplest generalization of the above memory function is to include the Maxwell relaxation time (τ_ν) and the Q-dependence of ω_0, which yields (Boon and Yip 1980)

$$M'(Q, \omega) = (1 - \gamma^{-1})(\gamma \omega_0^2 / Q^2) \gamma \chi Q^2 / [(\gamma \chi)^2 Q^4 + \omega^2] + \nu_1 / (1 + \omega^2 \tau_\nu^2) \tag{4a}$$

$$M''(Q, \omega) = -\omega (1 - \gamma^{-1})(\gamma \omega_0^2 / Q^2) / [(\gamma \chi)^2 Q^4 + \omega^2] - \nu_1 \omega \tau_\nu / (1 + \omega^2 \tau_\nu^2) \tag{4b}$$

where c^2 has been replaced by $\gamma \omega_0^2 / Q^2$ according to equation (2b). Equations (4a) and (4b) contain four parameters ($\gamma, \chi, \nu_1, \tau_\nu$) which may vary with Q, but with our data (see figure 1) it is not possible to separate out individual behaviours. It is known from previous work (section 1) that these data are sensitive to ν_1 and τ_ν and so we shall use these parameters to exhibit the observed Q-dependence in (for example) figure 3. The Q-dependence of all the parameters has been discussed by Youden (1992).

As indicated in section 1 the extended hydrodynamic description (see, for example, de Schepper and Cohen 1980, van Well and de Graaf 1985) is based on the kinetic theory description of $S(Q, \omega)$ for hard-sphere fluids in terms of an infinite sum of Lorentzians, where for $Ql < 1$ the structure is dominated by the first three terms. Hence in the low-Q region $S(Q, \omega)$ may be represented by

$$\frac{S(Q, \omega)}{S(Q)} = 1/\pi \operatorname{Re} \lim_{\epsilon \to 0} \left(\frac{A_{-1}(Q)}{s + s_{-1}(Q)} + \frac{A_0(Q)}{s + s_0(Q)} + \frac{A_{+1}(Q)}{s + s_{+1}(Q)} \right) \tag{5}$$

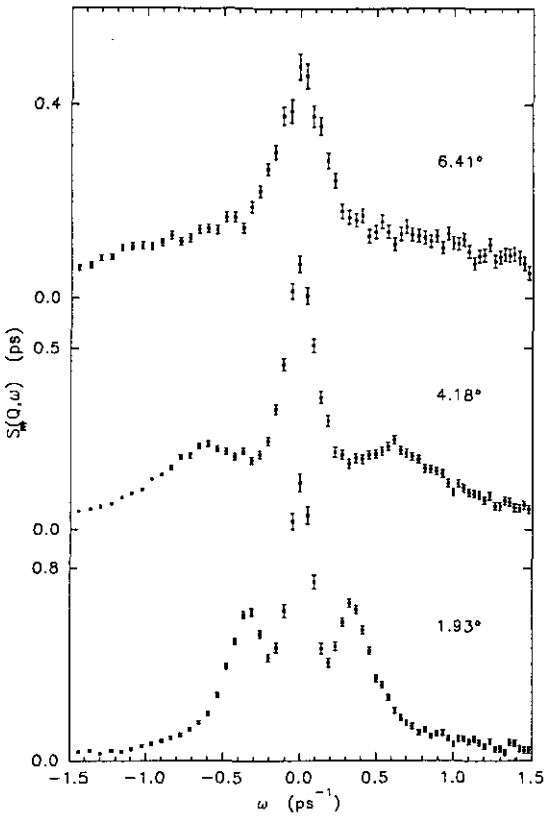

Figure 1. Examples of the observed $S_m(Q, \omega)$ at the constant scattering angles indicated on the figures, for the case of nitrogen gas at 295 K and 8.5 molecules nm^{-3}. A typical run took 15 hours and 15 spectra of the kind shown in this figure were obtained.

where $s = \epsilon + i\omega$, A_0, s_0 are real, and A_1, s_1 are either real or complex conjugate pairs. Higher-order terms in the infinite sum are only significant in the high-frequency wings. In the hydrodynamic limit these three modes go over to the one heat mode and the two sound modes of conventional hydrodynamics. The representation (5) allows a generalization of linearized hydrodynamics (equation (1)) which contains a Q-dependence in the thermodynamic and transport coefficients; the explicit relation between the two expressions is given by van Well and de Graaf (1985).

3. Experimental details

The neutron inelastic scattering experiments in the present study were performed on the IN5 TOF spectrometer at the High Flux Reactor of the Institut Laue–Langevin, Grenoble. These measurements in the low-Q region were made possible through the installation of a position-sensitive detector (0.64 m × 0.64 m) on the multichopper TOF spectrometer, and of additional shielding for this new detector. In addition a new electronic coding system was built, so that the x–y information from the 64 × 64 elements could be converted by hardware into concentric-ring information. Several possible beam centres were chosen, and for each a special circuit chip was designed.

At the start of an experiment the incident beam profile was measured using the full x–y detection system, and the true beam centre was adjusted, by moving the detector, so that it corresponded to the pre-selected value (usually the geometric centre or a point 0.15 m displaced). A cadmium disc was cut to the size of the incident beam and mounted on the detector so as to shield it from the transmitted neutron beam, which had a divergence of $\pm 0.3°$. Finally additional new shielding was installed to reduce the background to acceptable levels. The advantages of this apparatus are rapid, well resolved data collection at low values of Q.

The neutron flight path to the two-dimensional, position-sensitive detector was 3.820 m. The centre of the detector was shifted horizontally by 0.15 m from the position of the transmitted beam for most experiments, since this extended the upper limit of the momentum transfer range and provided a more uniform distribution of the detector elements over the angular range of interest. A further extension of the upper limit of Q would have been desirable (see section 5) but was not available. The response of the active area of the detector was coded into 10 mm wide annuli, for radii in the range from 0.05 m to 0.50 m giving a corresponding angular range from 0.8 to 7.3 degrees. At a later stage, to improve the counting statistics, the annuli were combined in threes giving a 30 mm width. The relative normalization of the detector rings was achieved using the scattering from a standard water sample, and the absolute cross-section normalization was estimated from the incoherent elastic scattering from the stainless steel sample cell for $Q > 1.0$ nm^{-1}.

For these experiments it is necessary that the neutron velocity, v_n, be significantly greater than the sound velocity, c, of the mode to be investigated, and the resolution less than the width of the central peak. For the present spectrometer these factors meant that moderately dense gases—such as nitrogen, at densities of the order of the critical density—could be studied in detail. In particular two states of nitrogen gas were studied at room temperature (3.2ϵ for LJ potential) with densities in units of molecules nm^{-3} of 8.5 (1.3× critical density) and 5.9 (0.9× critical density). The thermodynamic and transport properties for these two states are given in table 1. The final choices of incident wavelengths for the two samples were 0.50 nm and 0.56 nm or 3.27 and 2.61 meV, with energy resolutions of 109 μeV and 78 μeV (FWHM) respectively.

Under the present experimental conditions, the nitrogen molecule may be viewed as a rigid molecule: at room temperature the molecules are confined to their ground vibrational state—the fraction of molecules in higher states being 1.40×10^{-5} (Herzberg 1950). Furthermore, since the anisotropic forces are weak compared to the isotropic forces, a free rotation approximation would be reasonably valid (Sears 1966). In addition, through using a partial wave expansion of the scattering cross section in terms of the angular momentum transferred to the system, it can be seen that for low values of the momentum transfer Q, only the $l = 0$ spherical harmonic term is significant, giving (Sears 1966)

$$d^2\sigma/d\Omega\, d\omega = N(k_f/k_0)\{j_0^2(Qr_0/2)[4b_c^2 S_c(Q, \omega) + 2b_i^2 S_i(Q, \omega)]\} \qquad (6)$$

with b_c and b_i the bound atomic coherent and incoherent scattering lengths and r_0 the bond length. For nitrogen in the experimental range of Q up to 1.5 nm^{-1}, the spherical Bessel function $j_0^2(Qr_0/2)$ is essentially unity. Under these circumstances, the relative contributions of the coherent and incoherent dynamic structure factors are 0.978 and 0.022 respectively, so the coherent contribution is by far the more important.

Table 1. The thermodynamic and transport properties of the nitrogen samples.

			N_2[a,b]	N_2[a,b]
Pressure	P	(MPa)	46.1	27.3
Temperature	T	(K)	295.0	295.0
Density	ρ	(nm^{-3})	8.50	5.93
Speed of sound	c	($m\ s^{-1}$)	580.0	467.0
Ratio of specific heats	γ		1.702	1.709
Specific heat	C_p	($J\ kg^{-1}K^{-1}$)	1376	1348
Specific heat	C_v	($J\ kg^{-1}K^{-1}$)	808.4	788.4
Structure factor limit	$S(0)$		0.449	0.700
Thermal conductivity	λ	($W\ m^{-1}K^{-1}$)	0.0554	0.0432
Thermal diffusivity $\times\gamma$	χ	(nm^2ps^{-1})	0.173	0.199
Shear viscosity	η	(μPa s)	33.2	25.9
Bulk viscosity[c]	ζ_{ME}	(μPa s)	14.0	6.06
Longitudinal viscosity[d]	ν_l	(nm^2ps^{-1})	0.183	0.169
Self-diffusion[e]	D	($10^{-8}m^2\ s^{-1}$)	4.4	6.7

[a] Younglove (1982).
[b] Angus *et al* (1979).
[c] Hirschfelder *et al* (1954); Enskog calculation.
[d] $\nu_l = (4\eta/3 + \zeta)/\rho M$. Here ζ was approximated by $2\zeta_{ME}$ for N_2 where ME = modified Enskog.
[e] Chatelet *et al* (1983).

The higher-density nitrogen sample was contained in a stainless steel (304) cell, that was used previously in similar experiments (Egelstaff *et al* 1989). Tests conducted by Teixeria (1988) showed that the small-angle scattering for this vessel was basically confined to momentum transfers of less than 0.3 nm^{-1}, although it extended (at a low level) up to 1.0 nm^{-1}. Since the transmission of the cell could not be measured accurately at the IN5 spectrometer, it was estimated from the known scattering properties of the components of stainless steel 304. For the lower-density nitrogen, a steel cell with single-crystal sapphire windows (Bafile *et al* 1990) was used. Although this cell produced a considerably smaller background for these low-angle experiments, due to its geometry it unfortunately partially shielded neutrons that were scattered towards the outer annuli of the detector. The sample pressure and temperature were monitored throughout the course of the measurements. While the pressure was determined with an accuracy of about 0.1%, no active temperature control was used and the natural temperature fluctuations were 0.5 K or 0.2%. The corresponding densities were calculated using the published *PVT* data contained in the compilation by Younglove (1982), and were further checked against the data of Angus *et al* (1979).

Procedures for the computation of $S(Q, \omega)$ from neutron time-of-flight (TOF) data have been described previously, for example by Copley *et al* (1973), Verkerk and van Well (1985) or Egelstaff (1987). The general method accounts for the various experimental effects such as background, container scattering, detector response, attenuation and multiple scattering. For the present experiments at low Q, the attenuation factors were approximated by the energy-dependent transmission of the samples, where for the nitrogen the variation of the total cross section for low-energy neutrons was obtained from Melkonian (1949). Also, within the low-Q region the calculated multiple scattering had a very wide, flat, almost linear energy distribution, since it consisted mainly of double scattering through two large angles where the energy width of the spectra is relatively large. Hence this distribution was taken

to be linear across each spectrum, with the absolute level determined by matching the differential cross sections from the experiment and hydrodynamic theory in the large frequency regions where the single-scattering contribution is relatively small and varying smoothly. Although it is also in this energy region that the actual response of the fluid is likely to differ slightly from the low-Q theory of hydrodynamics, the intensity here is very small so this general level of multiple scattering is known sufficiently well to yield good results in the region of interest. The error in this procedure is estimated to be less than the other sources of error.

The differential cross section is related to the observable dynamic structure factor (denoted by S_m) through

$$S_m(Q, \omega) = (1/\langle b^2 \rangle)(\hbar/m)(t_f^4/t_0)\, \mathrm{d}^2\sigma/\mathrm{d}\Omega\, \mathrm{d}t_f \tag{7}$$

where t_0 and t_f are the TOFs of the incident and scattered radiation respectively. The experimental results—which obey the principle of detailed balance—were symmetrized by multiplying by $\exp(-\hbar\omega/2k_B T)$ in order to obtain effective classical data. As $\hbar\omega \ll k_B T$ the magnitude of the change in this case is small, being about 1%. Finally, for comparison with theoretical models, the spectra were converted from the constant-angle, constant-TOF grid, to a constant-momentum and constant-frequency grid using cubic spline interpolations.

4. Experimental results and theoretical models

The conservation of momentum and energy in the scattering process means that for a fixed angle both Q and ω are variables. Examples of the experimental $S(Q, \omega)$ measured at constant angle denoted by $S_m(Q, \omega)$, are shown in figure 1. After the raw data were combined into 30 mm wide annuli, the angular separation of experimental spectra was 0.45°. Afterwards these data were converted to the constant-Q format (denoted by S_0), and some results for the two states of nitrogen are shown in figure 2, (*a*)–(*d*). In transforming to constant Q the range over which complete spectra are obtained is restricted to a range of Q from roughly 0.5 to 1.5 nm^{-1}. The experimental points (with error bars) in figures 1 and 2, may be compared to theoretical curves which in addition to the contribution from the coherent $S(Q, \omega)$ as described by the above hydrodynamic models, also included a 2.2% contribution due to incoherent scattering. This latter part was assumed to be given by a Lorentzian centred at $\omega = 0$, with a full width at half maximum of $2D$, where D is the self-diffusion coefficient. Hence this contribution—with a width varying from one-fifth to twice the resolution width—slightly increased the intensity of the predicted $S_0(Q, \omega)$ in the central peak around $\omega = 0$. For the calculated $S_0(Q, \omega)$ presented here, the effect of the finite experimental resolution has been included approximately in the calculated data by convoluting the theoretical curves with a Gaussian shape representing the total resolution function. The exact function is nearer to a triangular shape, but it is not expected that the choice of other functions for the shape of the total instrumental resolution will affect the result significantly. For the comparison with theory a normalization factor, f_n was also included as an adjustable parameter to account for any minor inconsistencies in the areas of the theoretical and experimental profiles due to the uncertainty associated with the experimental absolute normalization.

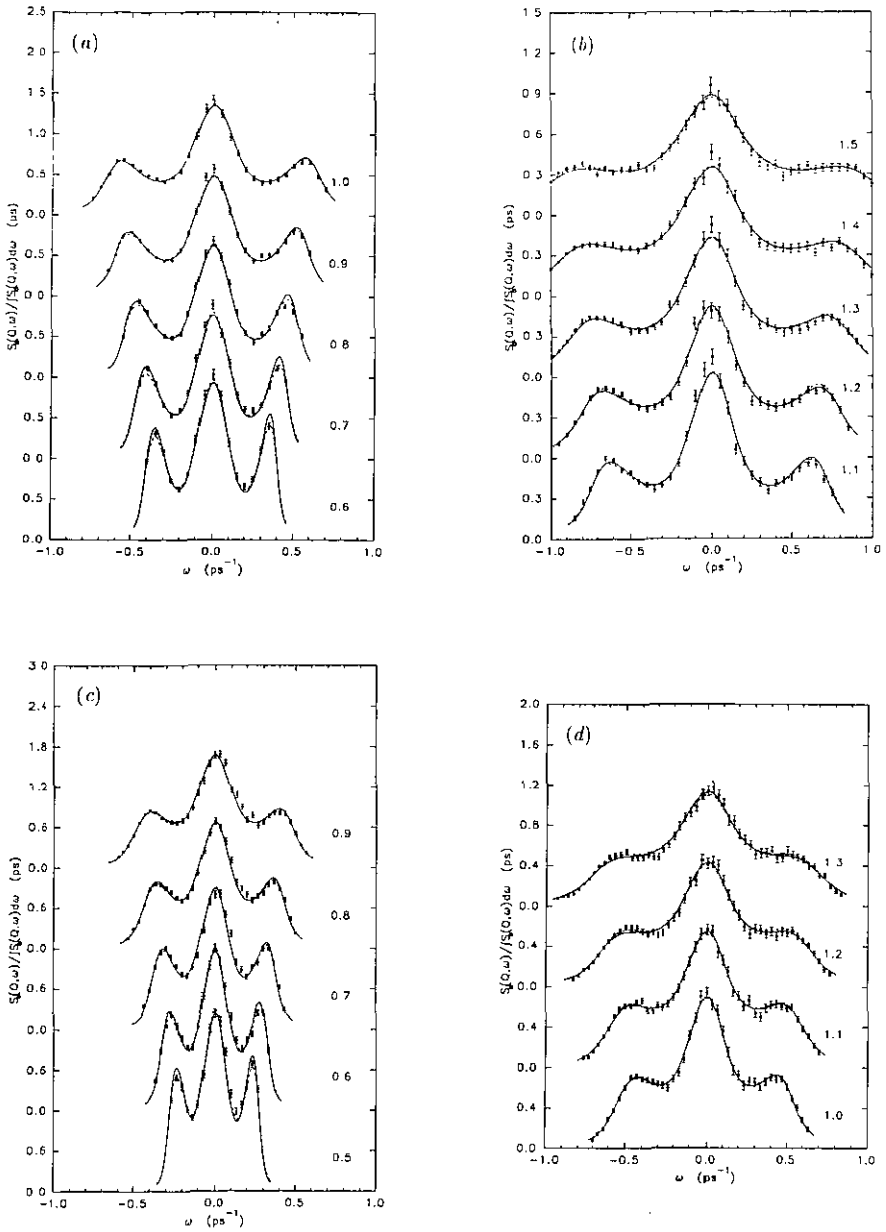

Figure 2. (*a*), (*b*) $S_0(Q, \omega)$ for N_2 at 8.5 nm^{-3}: experimental data (points with error bars) and hydrodynamic theory (equations (2) and (4)) with either the fitted (dashed curve) or the average (solid curve) values of ν_1 and τ_ν. The Q-values (in nm^{-1}) are indicated on the right-hand side, and theory has been folded with the experimental resolution function. (*c*), (*d*) as (*a*), (*b*) but for N_2 at 5.9 nm^{-3}.

The macroscopic thermodynamic and transport coefficients required in the calculation of $S_0(Q, \omega)$ from the hydrodynamic expressions were generally available from published data (see table 1). However, the bulk viscosity ζ and the self-diffusion D could not be found in the literature and therefore had to be estimated. The value

of the bulk viscosity was based on a modified Enskog calculation (Hirschfelder *et al* 1954), with the effect of the anisotropic forces estimated from the MD simulation of Hoheisel and Luo (1990) who used both isotropic and anisotropic intermolecular potentials. For their simulations they used either 108, or 32 particles where they found negligible size dependence. Their results for nitrogen gas at 250 and 400 K showed that the values of the shear viscosity η as calculated using the isotropic one-centre potential and the anisotropic two-centre potentials were in agreement with each other within the statistical uncertainties. It is worth noting too that the modified Enskog theory predicted the experimental η correctly. In contrast the MD results showed that for the bulk viscosity ζ the values approximately doubled on the introduction of the two-centre potential compared to the one-centre potential, and further increased by roughly 10% when the quadrupole interaction was included. Thus if the modified Enskog result for ζ is considered to be roughly equivalent to the spherical potential case, then the MD results imply that the value of ζ for the anisotropic case should be approximately double the modified Enskog value. Thus we chose a ζ which was twice this value.

The estimate of the self-diffusion coefficient was obtained through the scaling of hard-sphere calculations (Chen *et al* 1977) to the MD data of Alder *et al* (1970), as done previously by Chatelet *et al* (1983). Finally, the variation of $S(Q)$ at low Q was approximated by a Lorentzian function centred on $Q = 0$ with a width determined by an interpolation between the value of $S(0) = \rho k_B T \chi_T$ and the available experimental data at higher Q (Sullivan and Egelstaff 1981, Egelstaff *et al* 1984). This is a reasonable approximation to the theoretical shape, and the error in using it is negligible, as over the Q-range used here the departure from the value of $S(Q \rightarrow 0)$ is only a few per cent.

In the lower limit of the present experimental Q-range the wavelength of the fluctuations is of the order of 5 to 10 times greater than the Enskog mean free path, so $S(Q, \omega)$ approaches the $Q \rightarrow 0$ limit of linearized hydrodynamics where the three-Lorentzian description dominates. The generalized hydrodynamic expressions (equations (2) and (4)) were used as the basis for further descriptions since they yield the correct zero- and second-frequency moments through the dependence of ω_0 on $S(Q)$. In the upper region of Q, generalizations of the macroscopic parameters may be required to yield an accurate description of the observed $S(Q, \omega)$. Although in the present case this was done mainly through the generalization of the memory function to include the relaxation time as in equation (4), other possibilities were considered also. To explore the possibility of a Q-dependence in the macroscopic coefficients, as well as any discrepancies in the estimated parameters, various non-linear least-squares fits were performed with the thermodynamic and transport coefficients and the viscosity relaxation time as free parameters. The errors in the resulting fitted parameters were obtained from the variance–covariance matrix, and we note that the possibility of systematic errors was not included explicitly in this treatment.

5. Discussion for nitrogen

For both nitrogen samples, the observed $S_0(Q, \omega)$ are described quite well by the linearized hydrodynamic theory, with the inclusion of a Maxwell relaxation time in the memory function yielding slightly better agreement than that obtained from the

simple linearized theory alone. In figure 2 the observed $S_0(Q, \omega)$ are compared to the hydrodynamic expressions (2) and (4), with the values of both ν_l and τ_ν, and the normalization adjustment factor, obtained through least-squares fits (dashed curves). Also included in these figures are the $S_0(Q, \omega)$ (solid curves) as calculated from the same hydrodynamic expression, but using the weighted averages of the fitted values of ν_l (excluding those at the two lowest Q-values) and τ_ν, with the normalization adjustment f_n again obtained from least-squares criteria. The fitted values of the parameters are illustrated in figure 3, (*a*)–(*d*). It is notable that the values of the longitudinal viscosity, ν_l, are close to the macroscopic value estimated above. In figure 3, (*a*) and (*c*), they show a Q-dependence of roughly 20% for $0.5 < Q < 1.5$ nm^{-1}, and it should be remembered that all the Q-dependence in these data is being transferred to one parameter. Also in figure 3, (*b*) and (*d*), the fluctuations in the Maxwell relaxation time, τ_ν, are greater than the analytical errors, which reveals the probable size of various experimental errors on this quantity. Furthermore, in the lower Q-range the constant-Q data for $S_0(Q, \omega)$ typically contain only one or two points beyond the maximum in the propagating mode, and we find that using the respective average values of τ_ν of 0.16 or 0.27 does not increase the mean square deviation. It is evident from figure 2 that using the weighted averages of the fitted values of ν_l and τ_ν, rather than the fitted values for each particular Q, produces significant deviations only at the two lowest Q-values. The resulting discrepancies are of the order of the expected systematic differences between the measurements of the propagating modes at positive and negative ω, and hence are similar in size to the experimental errors. We are planning a more accurate experiment over a more extensive Q-range to resolve these issues, since with the limited time allocation on this instrument the whole of the required range could not be covered.

The average values of the fitted ν_l for the nitrogen at 8.5 and 5.9 nm^{-3} are respectively 0.188 nm^2 ps^{-1} and 0.191 nm^2 ps^{-1} yielding estimates for ζ of 30.2 μPa s and 18.3 μPa s. A comparison with table 1 shows that (for the higher density) this value of ζ is 2.2 times the Enskog value, which is within the range estimated previously. In contrast, for the lower density the observed value is three times the Enskog value and therefore larger than predicted. Thus either the effect of the anisotropy increases for the lower-density nitrogen, or alternatively further generalizations in the hydrodynamic description should be considered. Ideally the macroscopic limit for ζ could be checked by Brillouin light scattering measurements in the $Q \to 0$ hydrodynamic regime. It is worthwhile to note that for the hard-sphere fluid at high density, where the hydrodynamic relaxation times are no longer extremely long and the relaxation time for the viscosity is still significant, the resulting $S(Q, \omega)$ at intermediate Q-values requires an ω-dependent generalization of the viscosity. Figure 3 shows that the Q-dependence of ν_l is probably significant and that its dependence is similar to that found for the lower-density argon case (section 6).

6. Discussion for argon

In addition to the experiments on the dense nitrogen samples reported here, experiments on argon gas at 295 K using the same spectrometer were performed by Bafile *et al* (1990)—see table 2 for the experimental conditions. This group converted their data to $S(Q, \omega)$ by deconvoluting the experimental resolution function. They

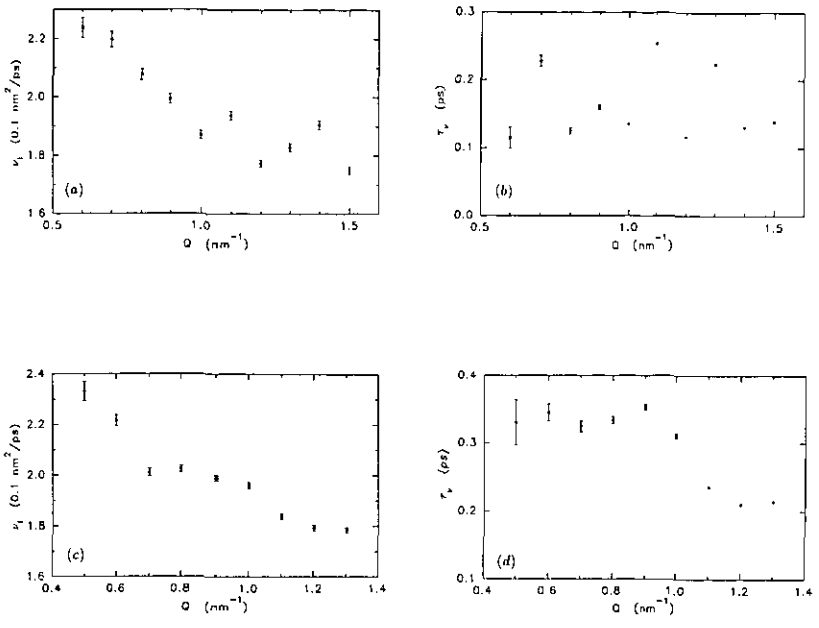

Figure 3. The fitted values of ν_l and τ_ν (defined in equations (1) and (4) respectively) for nitrogen at 295 K and used for the theoretical curves of figure 2. The errors shown in these figures are derived from the least-squares analysis, and the fluctuations in the data reflect the errors in the experimental data. (*a*) ν_l for nitrogen at 8.5 molecules nm^{-3}. The macroscopic value is 1.83×0.1 nm^2 ps^{-1}. (*b*) τ_ν for nitrogen at 8.5 molecules nm^{-3}. (*c*) ν_l for nitrogen at 5.9 molecules nm^{-3}. The macroscopic value is 1.69×0.1 nm^2 ps^{-1}. (*d*) τ_ν for nitrogen at 5.9 molecules nm^{-3}.

interpreted their results in terms of the extended hydrodynamic model, concluding that $S(Q, \omega)$ from the region of the three hydrodynamic modes to much larger Q, may be described in terms of the three extended modes.

Table 2. The thermodynamic and transport properties of the argon samples of Bafile *et al* (1990).

			^{36}Ar[a]	^{36}Ar[a]
Pressure	P	(MPa)	200.85	80.35
Temperature	T	(K)	301.5	301.5
Density	ρ	(nm^{-3})	5.04	2.00
Speed of sound	c	(m s^{-1})	393.0	353.0
Ratio of specific heats	γ		2.211	1.905
Structure factor limit	$S(0)$		0.997	1.066
Thermal diffusivity $\times\gamma$	χ	(nm^{2}ps^{-1})	0.259	0.514
Longitudinal viscosity[b]	ν_l	(nm^{2}ps^{-1})	0.139	0.267

[a] Values as obtained by Bafile *et al* (1990) from Rabinovich *et al* (1988).
[b] $\nu_l = (4\eta/3 + \zeta)/\rho M$. Here ζ was approximated by ζ_{ME} (Hirschfelder *et al* 1954), which yielded values of 0.12η and 0.020η for the two densities.

The $S(Q, \omega)$ for argon at the higher density of 5.04 nm^{-3} can be equally well described by the generalized hydrodynamic expressions (2) and (4), as shown in

figure 4. Here the relaxation time τ_ν (0.86 ps) is the average value of the least-squares fitted results. In other respects, the calculation used the known values of the macroscopic parameters (Rabinovich *et al* 1988)—including ν_1 which again relied on the modified Enskog value of ζ. The low-Q behaviour of $S(Q)$ was obtained from a virial series calculation (Ram *et al* 1982). At the lowest Q, where the width of $S(Q, \omega)$ was too small for the resolution deconvolution to be accurate (Bafile *et al* 1990), the experimental $S(Q, \omega)$ is fairly well described by linearized hydrodynamics. At the higher Q-values, one must include the generalization to a non-vanishing relaxation time τ_ν. Only at the highest Q, however, is there an indication that the damping of the propagating mode, given by the macroscopic τ_1 and the average τ_ν, is slightly too large.

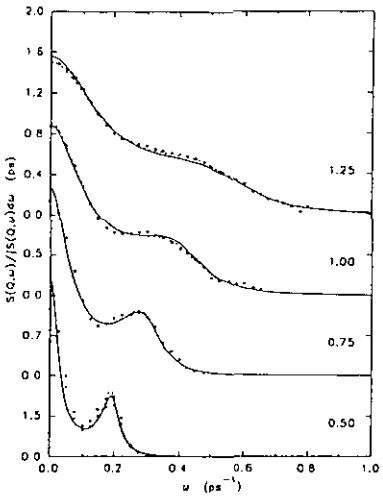

Figure 4. $S(Q, \omega)$ for ^{36}Ar at 5.04 nm^{-3}: experimental data (solid squares) and hydrodynamic theory with either the fitted values of ν_1 and τ_ν (dashed curve), or the macroscopic value of ν_1 and the averge value of τ_ν (solid curve). The Q-values (in nm^{-1}) are indicated on the right hand side. In the case of $Q = 0.5$ nm^{-1} the experimental data (triangles) with the same normalization as for the larger Q data are shown, together with (squares) data obtained using the self-normalization.

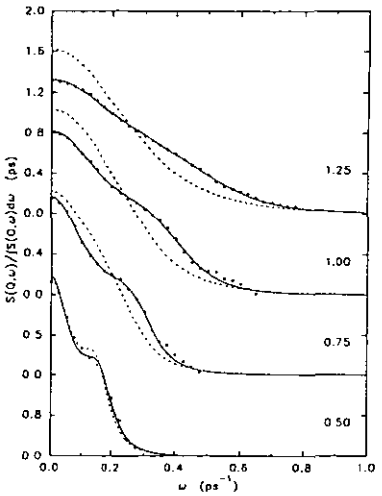

Figure 5. $S(Q, \omega)$ for ^{36}Ar at 2.00 nm^{-3}: experimental data (solid squares) and hydrodynamic theory with the fitted values of ν_1 and τ_ν (solid curve). Also shown is the linearized hydrodynamic theory (equation (1)) (dashed curve). The Q-values (in nm^{-1}) are indicated on the right hand side.

For the much lower argon density of 2.00 nm^{-3}, the wavelength of the fluctuations is of the order of the Enskog mean free path, and $S(Q, \omega)$ can be explained in terms of the generalized expression (2) plus (4) only if ν_1 and τ_ν vary with Q: i.e. $2.8 > \nu_1 > 2.0 \times 10^{-1}$ nm^2 ps^{-1} and $2.5 > \tau_\nu > 1.0$ ps for $0.5 < Q < 1.3$ nm^{-1}. The agreement between the experimental $S(Q, \omega)$ and the hydrodynamic theory with the least-squares fitted values of ν_1 and τ_ν is illustrated in figure 5. The pronounced deviations from the linearized hydrodynamic theory that occur in this case imply that the propagating modes persist to a much greater extent than predicted by the simple $Q \rightarrow 0$ theory. It should be noted that the above analyses may not be unique,

since the degree of correlation among the various parameters is particularly large in this case, which prevents unambiguous conclusions from being made about the behaviour of each generalized coefficient. In this respect both neutron and light Brillouin scattering investigations suffer from a common difficulty.

7. Concluding remarks

It is interesting to note that the flexibility offered by neutron scattering allows both the variation of Q for a given state and the variation of state for a given Q to be studied. The experiments on nitrogen and argon illustrate these two approaches respectively. It is not obvious that both kinds of experiment will test hydrodynamic theory in the same way, but with the present limitations to the data this question may not be examined adequately.

An estimate for τ_ν may be found from the equal-relaxation-time approximation (Egelstaff 1967): $\tau_\nu = \nu_1/2c^2$. The calculated estimates for all the above samples are contained in table 3, along with the corresponding values determined from the experimental $S(Q, \omega)$, and we note that there is an obvious similarity between the two sets of values. To obtain an overall perspective of the various samples that have been studied in the transition region, it is useful to consider the characteristic length (y) and frequency (x/y) parameters of the fluctuations. The parameter y may be estimated from the hard-sphere expression $y = \pi\sqrt{2}\rho\sigma^2 g(\sigma)/Q$ and $x = \omega\sqrt{2}Qv_0$ where σ is the equivalent hard-sphere diameter and $g(\sigma)$ the pair-correlation function on contact. While the concept of a mean free path is not strictly valid for dense fluids with continuous intermolecular potentials, the above simple calculations nevertheless provided representative values of y and x/y for the current comparisons (table 4). In the lower range of the experimentally accessible Q-values, both nitrogen samples approach the hydrodynamic regime with $y > 6$ and $x/y < 0.2$. Over the experimental Q-range these two samples, as well as the higher-density argon, are in the transition region of y and x/y approaching one. In contrast, the lower-density argon is already in the transition region at the lowest Q, and then further extends into the kinetic regime of $y < 1$ and $x/y > 1$. A detailed theoretical discussion of departures from hydrodynamic theory observed here is beyond the scope of this paper.

Table 3. The estimates for the relaxation time τ_ν. (Calculated value is $\tau_\nu \sim \nu_1/2c^2$. Experimental value is the average over Q of the fitted values.)

	N_2	N_2	Ar	Ar
Density (nm^{-3})	8.5	5.9	5.0	2.0
Calculated: τ_ν(ps)	0.28	0.44	0.47	1.1
Experimental: τ_ν (ps)	0.16	0.27	0.86	2.3–1.2

In conclusion, it is evident that in the experimental range of y and x/y considered here, $S(Q, \omega)$ is described by the generalization of linearized hydrodynamics to include the Maxwell relaxation time τ_ν. These effects imply that the first deviation from the linearized theory is the persistence of the propagation of the longitudinal sound modes, as has been noted previously (for example, Boon and Yip 1980 and the references therein). For the lower-density argon, for which both the wavelength and

Table 4. The estimates for the parameters y and x/y.

Density (nm^{-3})	N_2 8.5	N_2 5.9	Ar 5.0	Ar 2.0
y (0.5 nm^{-1})	11.0	6.5	3.6	1.4
(1.3 nm^{-1})	4.3	2.5	1.4	0.5
x/y (for $\omega = cQ$) (0.5 nm^{-1})	0.1	0.2	0.3	0.7
(1.3 nm^{-1})	0.3	0.4	0.8	1.8

the frequency of the fluctuations further extend beyond the hydrodynamic limit, the generalization must include a Q-dependence in τ_ν, and possibly a slight dependence in ν_1.

The correlations that exist among the various parameters in the generalized hydrodynamic description prevent the behaviour of these parameters from being unambiguously determined from $S(Q, \omega)$ at this stage. However, the generalization to (Q, ω) dependent thermodynamic and transport coefficients can be obtained from MD simulations, with comparisons to $S(Q, \omega)$ then providing an opportunity for further examination of the behaviour in the transition regime. Obviously, this approach can be used to examine the generalized coefficients in the extended hydrodynamics model as well. As our techniques are developed to give higher precision and an extended Q-range, we expect that this approach will yield a much greater insight into the macroscopic dynamics of fluids.

Acknowledgments

We would like to acknowledge the financial help of the Natural Sciences and Engineering Research Council of Canada, and the technical help of the staff of the Institut Laue–Langevin. We are grateful to Dr P Verkerk for graphs of the data published by Bafile *et al* (1990).

References

Ailawadi N K, Rahman A and Zwanzig R 1971 *Phys. Rev.* A **4** 1616
Alder B J, Gass D and Wainwright T E 1970 *J. Chem. Phys.* **53** 3813
Alley W E and Alder B J 1983 *Phys. Rev.* A **27** 3158
Alley W E, Alder B J and Yip S 1983 *Phys. Rev.* A **27** 3174
Angus S, de Reuck K M and Armstrong B 1979 *International Thermodynamic Tables of the Fluid State 6: Nitrogen* (Oxford: Pergamon)
Bafile U, Verkerk P, Barocchi F, de Graaf L A, Suck J-B and Mutka H 1990 *Phys. Rev. Lett.* **65** 2394
Bell H G, Kollmar A, Alefeld B and Springer T 1973 *Phys. Lett.* **45A** 479
Bell H, Moeller-Wenghoffer H, Kollmar A, Stockmeyer R, Springer T and Stiller H 1975 *Phys. Rev.* A **11** 316
Boon J P and Yip S 1980 *Molecular Hydrodynamics* (New York: McGraw-Hill)
Carneiro K, Nielsen M and McTague J P 1973 *Phys. Rev. Lett.* **30** 481
Chatelet M, Kieffer J and Oksengorn B 1983 *Chem. Phys.* **79** 413
Chen S H, Postol T A and Sköld K 1977 *Phys. Rev.* A **16** 2112
Chung C-H and Yip S 1969 *Phys. Rev.* **182** 323
Clark N A 1975 *Phys. Rev.* A **12** 232
Copley J R D, Price D L and Rowe J M 1973 *Nucl. Instrum. Methods* **107** 501
Copley J R D and Rowe J M 1974a *Phys. Rev.* A **9** 1656
—— 1974b *Phys. Rev. Lett.* **32** 49

Dasannacharya B A, Kollmar A and Springer T 1976 *Phys. Lett.* **55A** 337
de Schepper I M and Cohen E D G 1980 *Phys. Rev.* A **22** 287
de Schepper I M, van Rijs J C, van Well A A, Verkerk P, de Graaf L A and Bruin C 1984 *Phys. Rev.* A **29** 1602
de Schepper I M, Verkerk P, van Well A A and de Graaf L A 1983 *Phys. Rev. Lett.* **50** 974
Egelstaff P A 1967 *An Introduction to the Liquid State* (New York: Academic)
—— 1987 *Neutron Scattering* vol 2, ed K Sköld and D L Price (New York: Academic)
Egelstaff P A, Hawkins R K, Litchinsky D, Lonngi P A and Suck J-B 1984 *Mol. Phys.* **53** 389
Egelstaff P A, Kearley G, Suck J-B and Youden J P A 1989 *Europhys. Lett.* **10** 37
Herzberg G 1950 *Molecular Spectra and Molecular Structure* (Princeton, NJ: van Nostrand)
Hirschfelder J O, Curtiss C F and Bird R B 1954 *Molecular Theory of Gases and Liquids* (New York: Wiley)
Hoheisel C and Luo H 1990 *Nuovo Cimento* D **12** 499
Kadanoff L P and Martin P C 1963 *Ann. Phys., NY* **24** 419
Levesque D, Verlet L and Kurkijarvi J 1973 *Phys. Rev.* A **7** 1690
Melkonian E 1949 *Phys. Rev.* **76** 1750
Mountain R D 1976 *Adv. Mol. Relax. Process.* **9** 225
Nelkin M and Yip S 1966 *Phys. Fluids* **9** 380
Postol T A and Pelizzari C A 1978 *Phys. Rev.* A **18** 2321
Rabinovich V A, Vasserman A A, Nedostup V I and Veksler L S 1988 *Thermophysical Properties of Neon, Argon, Krypton, and Xenon* (Washington, DC: Hemisphere)
Rahman A 1974a *Phys. Rev.* A **9** 1667
—— 1974b *Phys. Rev. Lett.* **32** 52
Ram J, Barker R, Cummings P T and Egelstaff P A 1982 *Phys. Chem. Liq.* **11** 315
Sears V F 1966 *Can. J. Phys.* **44** 1279
—— 1969 *Can. J. Phys.* **47** 199
—— 1970 *Can. J. Phys.* **48** 616
Söderström O, Copley J R D, Suck J-B and Dorner B 1980 *J. Phys. F: Met. Phys.* **10** 151
Sullivan J D and Egelstaff P A 1981 *Mol. Phys.* **44** 287
Teixeria J 1988 private communication
van Hove L 1954 *Phys. Rev.* **95** 249
van Well A A and de Graaf L A 1985 *Phys. Rev.* A **32** 2396
Verkerk P and van Well A A 1985 *Nucl. Instrum. Methods Res. Phys.* A **228** 438
Woods A D B, Martel P and Svensson E C 1978a *Neutron Inelastic Scattering 1977* vol 2 p 37 (Vienna: IAEA)
—— 1978b *Can. J. Phys.* **56** 302
Youden J 1992 *PhD Thesis* University of Guelph, Canada
Younglove B A 1982 Thermophysical properties of fluids I *J. Phys. Chem. Ref. Data* **11**
Zwanzig R 1967 *Phys. Rev.* **156** 190